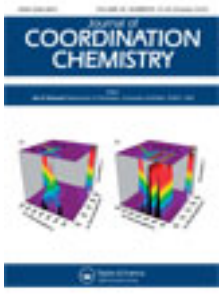

Journal of Coordination Chemistry
Publication details, including instructions for authors and subscription information:
http://www.tandfonline.com/loi/gcoo20

A paramagnetic octahedral trans-dihydroxy chromium(IV) complex with dianionic tetradentate Schiff base salophen and crystal structure of its trans-diisothiocyanato analog

Manjuri K. Koley [a], Seshadri C. Sivasubramanian [b], Babu Varghese [c], Periakaruppan T. Manoharan [d] & Aditya P. Koley [e]

[a] Department of Chemical Engineering, Birla Institute of Technology and Science-Pilani, K.K. Birla Goa Campus, Zuarinagar 403726, Goa, India

[b] Department of Chemistry, Birla Institute of Technology and Science-Pilani, Pilani Campus, Pilani 333031, Rajasthan, India

[c] Sophisticated Analytical Instruments Facility, Indian Institute of Technology-Madras, Chennai 600 036, Tamil Nadu, India

[d] Department of Chemistry, Indian Institute of Technology-Madras, Chennai 600 036, Tamil Nadu, India

[e] Department of Chemistry, Birla Institute of Technology and Science-Pilani, K.K. Birla Goa Campus, Zuarinagar 403726, Goa, India

Accepted author version posted online: 14 Aug 2012.Published online: 06 Sep 2012.

To cite this article: Manjuri K. Koley, Seshadri C. Sivasubramanian, Babu Varghese, Periakaruppan T. Manoharan & Aditya P. Koley (2012) A paramagnetic octahedral trans-dihydroxy chromium(IV) complex with dianionic tetradentate Schiff base salophen and crystal structure of its trans-diisothiocyanato analog, Journal of Coordination Chemistry, 65:20, 3623-3640, DOI: 10.1080/00958972.2012.720978

To link to this article: http://dx.doi.org/10.1080/00958972.2012.720978

Journal of Coordination Chemistry
Vol. 65, No. 20, 20 October 2012, 3623–3640

A paramagnetic octahedral *trans*-dihydroxy chromium(IV) complex with dianionic tetradentate Schiff base salophen and crystal structure of its *trans*-diisothiocyanato analog

MANJURI K. KOLEY†, SESHADRI C. SIVASUBRAMANIAN‡, BABU VARGHESE§, PERIAKARUPPAN T. MANOHARAN*¶ and ADITYA P. KOLEY*‖

†Department of Chemical Engineering, Birla Institute of Technology and Science-Pilani, K.K. Birla Goa Campus, Zuarinagar 403726, Goa, India
‡Department of Chemistry, Birla Institute of Technology and Science-Pilani, Pilani Campus, Pilani 333031, Rajasthan, India
§Sophisticated Analytical Instruments Facility, Indian Institute of Technology-Madras, Chennai 600 036, Tamil Nadu, India
¶Department of Chemistry, Indian Institute of Technology-Madras, Chennai 600 036, Tamil Nadu, India
‖Department of Chemistry, Birla Institute of Technology and Science-Pilani, K.K. Birla Goa Campus, Zuarinagar 403726, Goa, India

(*Received 19 June 2012; in final form 24 July 2012*)

A paramagnetic octahedral *trans*-dihydroxychromium(IV) complex, $[Cr(OH)_2(salophen)]$ (**1**) (H_2salophen = *N*,*N*′-bis(salicylidene)-1,2-phenylenediamine), has been synthesized and characterized by elemental analysis, magnetic moment measurement, IR, UV-Vis, and EPR spectroscopic studies. Measured room temperature (RT) magnetic moment value is 2.79 BM for **1**, indicating a d^2 ($S = 1$) system with a triplet ground state. Compound **1** exhibits powder EPR spectra at RT and LNT, which show the allowed transition $\Delta M_s = \pm 1$ ($g = 2.0038$) as well as the "forbidden" half-field transition ($\Delta M_s = \pm 2$) at $g = 4.2080$. Two successive reduction waves are observed in the cyclic voltammogram of **1** in CH_3CN at −0.84 and −1.63 V (*vs.* Ag/AgCl), respectively. Compound **1** readily reacts with Mn^{2+} ion, a Cr(IV)–specific reductant and also undergoes –OH substitution reactions in solution with NCS^- and imidazole. The *trans*-diisothiocyanato analog, $[Cr(NCS)_2(salophen)]$ (**2**), with $\mu_{eff} = 2.80$ BM has been structurally characterized by X-ray crystallography and found to contain two N-bonded axial thiocyanato ligands with slightly different axial Cr–N bond lengths (N(3)–Cr(1), 2.032(2); N(4)–Cr(1), 2.015(2) Å). Compound **2** and the corresponding Cr(III) compound $K[Cr(NCS)_2(salophen)] \cdot H_2O$ (**3**) show significant difference in their electronic structures as revealed from their electronic spectra.

Keywords: Chromium(IV) complex; ONNO donor salophen; EPR and electronic spectra; Cyclic voltammetry; X-ray crystallography

*Corresponding authors. Email: ptm@iitm.ac.in; koleyap@yahoo.co.in

Journal of Coordination Chemistry
ISSN 0095-8972 print/ISSN 1029-0389 online © 2012 Taylor & Francis
http://dx.doi.org/10.1080/00958972.2012.720978

1. Introduction

Cr(III) Schiff base complexes involving H_2salen (*N*,*N*′-bis(salicylidene)-ethylenediamine) and H_2salophen (*N*,*N*′-bis(salicylidene)-1,2-phenylenediamine) (and related ligands derived from different substituted salen or salophen) are widely used in catalysis of various organic reactions such as alcohol oxidations [1], alkene epoxidations [2, 3], asymmetric epoxidations [4–6], kinetic resolution of epoxides [7, 8], enantioselective additions of allyl organometallic reagents to aldehydes [9–11] and ring-opening polymerization [12]. Also, these Cr(III) Schiff-base complexes are used in construction of artificial metalloenzymes [13–15] in bioinorganic chemistry. These artificial metalloenzymes are able to catalyze enantioselective sulfoxidation of specific organic substrates. These Cr(III) Schiff-base compounds are capable of catalyzing oxygen atom transfer from reagents such as iodosylbenzene and H_2O_2. to various organic substrates [2, 3, 16–18]. From mechanistic studies of these oxygen atom transfer reactions it is shown that, initially a $[Cr^{V}O(\text{Schiff base})]^{+}$ complex is formed from reaction of e.g., iodosylbenzene and the Cr(III) Schiff-base complex and then there is an electrophilic attack on the substrate by this oxochromium(V) cation. Adam *et al*. [16] have suggested from their mechanistic studies of chemoselective oxidation of alcohols to carbonyl products with iodosobenzene diacetate mediated by chromium(III)salen complexes that a $[Cr^{IV}(OAc)(salen)]^{+}$ species other than the $[Cr^{V}O(salen)]^{+}$ complex may be involved in the catalytic oxidation.

Many $[Cr^{V}O(salen)]^{+}$ complexes are synthesized from the corresponding $[Cr^{III}(salen)]^{+}$ complexes and their properties have been studied [2, 3, 16–18]. Srinivasan and Kochi [3] have reported the synthesis and molecular structures of a number of stable oxochromium(V)salen cations from the corresponding Cr(III)salen cations treated with a slight excess of iodosylbenzene. However, they found that the Cr(III)salophen complex, when treated with iodosylbenzene in CH_3CN, yielded a transient dark-green–black solution presumably due to the formation of an oxochromium(V)salophen cation as indicated from its EPR spectrum. This dark green–black solution was unstable and precipitated a brown solid. This sparingly soluble brown solid was suspected by the authors [3] to be an oxochromium(IV) species. No further information was available on this compound. This prompted us to synthesize and characterize a Cr(IV) compound with salophen.

Reports of Cr(IV) species are more common as short lived transient intermediates during reduction of various Cr(VI) complexes, apart from a considerable number of chromium(IV) compounds that have been isolated in the solid state and characterized [19–24]. Recently we reported the synthesis and characterization of two stable paramagnetic octahedral chromium(IV) bischelate complexes with dianionic tridentate SNO donor Schiff-base ligands [23] and an oxochromium(IV) complex with dianionic tetradentate ONNO donor salen [24]. Following a similar method of preparation, we are able to stabilize and isolate another Cr(IV) compound which was initially thought to be a *trans*-aqua oxochromium(IV)salophen compound as initially reported [24], but turns out to be its tautomer *trans*-dihydroxy chromium(IV)salophen $[Cr(OH)_2(\text{salophen})]$ (**1**). Here, we report the synthesis, magnetic, spectroscopic, and electrochemical properties as well as the reactivity of this compound in solution. The analogous diisothiocyanato complex, $[Cr(NCS)_2(\text{salophen})]$ (**2**), has been structurally characterized by X-ray crystallography. To the best of our knowledge this is the first report of a highly stable paramagnetic *trans*-dihydroxy chromium(IV) compound that is

isolated in the solid state and its *trans*-diisothiocyanato chromium(IV) analog characterized by X-ray crystal structure. The corresponding Cr(III) complex, $K[Cr(NCS)_2(salophen)] \cdot H_2O$ (**3**), has also been synthesized and its spectroscopic properties are studied in order to get insight in the difference in its electronic structure with that of **2** presumably containing the metal ion in +4 oxidation state.

2. Experimental

2.1. *General remarks*

Cr compounds are carcinogenic. Necessary precautions must be taken to avoid skin contact and inhalation of their solutions and dusts.

2.2. *Materials*

o-Phenylenediamine was obtained from Sigma and used without purification. Salicylaldehyde, triphenyl phosphine, and imidazole were obtained from Aldrich and absolute ethanol (GR) was obtained from Merck, Germany. Potassium dichromate (GR) was obtained from Sarabhai Chemicals, India. Methanol (GR), dichloromethane (GR), toluene (GR), DMF (GR), acetonitrile (HPLC), and potassium thiocyanate (reagent grade) were obtained from Merck, India. All other chemicals were of reagent grade and used as received. Tetraethyl ammonium perchlorate (TEAP) was prepared using a method described [25].

2.3. *Synthesis of H_2salophen*

A solution of salicylaldehyde (6.1 g, 0.05 mol) dissolved in 15 mL of absolute ethanol was slowly added to a solution of *o*-phenylenediamine (2.7 g, 0.025 mol) dissolved in 35 mL of dry ethanol with constant stirring at room temperature (RT). The solution became hot. This was stirred for half an hour, when an orange compound separated from the solution. This was filtered, washed with ethanol, dried in vacuum and collected. The compound was recrystallized from ethanol. Anal. Calcd for $C_{20}H_{16}N_2O_2$ (%): C, 75.94; H, 5.10; N, 8.85. Found (%): C, 76.00; H, 5.12; N, 8.80. M.p. 167–168°C. UV-Vis (CH_3CN) [λ_{max}, nm ($\varepsilon \times 10^{-3}$ mol L^{-1} cm^{-1})]: 368 (13.4), 331 (22.8), 268 (29.75), 229 (33.74), 209 (40.25). IR (KBr pellet, cm^{-1}): 3450m, br ν(O–H); 1610s, ν(C=N); 1276s, ν(C–O).

2.4. *Synthesis of [$Cr(OH)_2$(salophen)] (1)*

A sample of solid potassium dichromate (0.294 g, 1 mmol) was added to a solution of H_2salophen (0.632 g, 2 mmol) dissolved in 50 mL of CH_3OH with constant stirring at RT. Stirring was continued for 72 h while the solution turned from yellow orange to red brown. The solution was filtered through a G4 sintered glass crucible and the red–brown filtrate (pH ~8) was evaporated to dryness in vacuum. The dark solid thus obtained was stirred at RT with 50 mL of a mixture of $CH_3CN : CH_2Cl_2$ (2 : 1)

and filtered. The red–brown filtrate was kept for slow evaporation at RT when a dark black–brown compound was obtained. This was filtered and washed thoroughly with toluene and dried. This compound was then recrystallized from CH_3CN–toluene (1 : 1) solution. Anal. Calcd for $C_{20}H_{16}N_2O_4Cr$ (%): C, 60.00; H, 4.03; N, 7.00. Found (%): C, 60.32; H, 4.10; N, 7.13. IR (KBr pellet, cm^{-1}): 3400m, br ν(O–H); 1605s, ν(C=N); 448m ν(Cr–N); 399m, 385m, br ν(Cr–O) [26].

2.5. *Synthesis of [Cr(NCS)$_2$(salophen)] (2)*

[Cr(OH)$_2$(salophen)] (**1**) (100 mg, 0.25 mmol) was dissolved in ~50 mL of CH_3OH in a stoppered conical flask by stirring the solution at RT. To this dry solid, KSCN (97.18 mg, 1.00 mmol) was added and stirring was continued for 12 h at RT. This solution was left for slow evaporation at ~20°C while dark reddish brown crystals resulted within 3–4 d. These were filtered using a G-4 sintered glass crucible and washed rapidly with cold CH_3CN and air dried. Finally, these crystals were thoroughly washed with water and dried in vacuum. Purification of this product was then performed by column chromatography on silica gel using a 3 : 1 mixture of CH_3CN–CH_2Cl_2 and the resulting red–brown complex was recrystallized from CH_3CN–toluene (2 : 1) as reddish–brown powder. Anal. Calcd for $C_{22}H_{14}N_4O_2S_2Cr$ (%): C, 54.76; H, 2.92; N, 11.61. Found (%): C, 55.02; H, 2.98; N, 11.73. UV-Vis (CH_3CN) [λ_{max}, nm ($\varepsilon \times 10^{-3}$ mol L^{-1} cm^{-1})]: 580 (0.091), 473 (3.454), 367 (11.910), 330 (17.872), 316 (18.561), 300 (22.054), 291 (24.466), 270 (26.260), 238 (34.269), 229 (36.673). IR (KBr pellet, cm^{-1}): 2104vs and 2088sh ν(CN); 1607s, ν(C=N); 450 m ν(Cr–N); 400 m, ν(Cr–O) [26].

Several attempts to grow single crystals by redissolving this recrystallized powder in different solvents and using various techniques were unsuccessful, so crystals directly obtained from the reaction of **1** with KSCN in methanol were used for X-ray crystallography. It was found that this compound cocrystallized with an unknown organic cluster whose structure we could not solve.

2.6. *Synthesis of K[Cr(NCS)$_2$(salophen)]·H$_2$O (3)*

[Cr(OH$_2$)$_2$(salophen)]NO_3 was prepared following a method described [27–29]. This compound (0.464 g, 1 mmol) was then dissolved in about 75 mL of methanol and reacted with four-fold excess of KSCN (0.389 g, 4 mmol) at RT for 24 h. The solution was filtered through a G-4 sintered glass crucible and the red–brown filtrate was left for slow evaporation at RT when dark red–brown compound separated. This was filtered and washed with cold methanol and air dried. Then the compound was thoroughly washed with water, dried *in vacuo* and recrystallized from CH_3CN : CH_2Cl_2 (1 : 1) solution. Anal. Calcd for $C_{22}H_{16}N_4O_3S_2CrK$ (%): C, 48.97; H, 2.99; N, 10.38. Found (%): C, 49.22; H, 3.10; N, 10.63. UV-Vis (CH_3CN) [λ_{max}, nm ($\varepsilon \times 10^{-3}$ mol L^{-1} cm^{-1})]: 600 (0.099), 578 (0.129), 464 (2.842), 375 (3.496), 328 (16.328), 316 (19.122), 290 (21.430), 281 (21.720), 235 (23.255). IR (KBr pellet, cm^{-1}): 2079s ν(CN); 1608s, ν(C=N).

2.7. *Reactions of [Cr(OH)$_2$(salophen)] (1)*

Reactions of **1** in CH_3OH solutions were carried out at RT and monitored spectrophotometrically after adding two fold excess of solid imidazole or KSCN or $Mn(OAc)_2$. In case of reaction with KSCN, it was also monitored by measuring the pH of $\sim$1 mmol L^{-1} solution of **1** in methanol before and after adding two fold excess of solid KSCN using a pH meter. The pH of the solution increases by almost one unit, and the final pH was $\sim$8. Also, we carried out the Mn^{2+} catalyzed disproportionation of [Cr(NCS)$_2$(salophen)] (**2**) and also that of $[Cr(imz)_2(salophen)]^{2+}$ (**4**); this latter species was generated *in situ* from reaction of [Cr(OH)$_2$(salophen)] with imidazole (1 : 2) in CH_3OH at RT, and monitored by the spectral change using UV-Vis spectroscopy. For PPh_3, solid reagent was added to the CH_3CN solution of **1** at RT and the spectrum was recorded. No spectral change in the visible region was noticed. Then, this solution was heated for 10 min and cooled, but still there was no spectral change observed in the visible region. Separation followed by purification of the components from the solution revealed unreacted **1** and PPh_3 as suggested from their IR and electronic spectra.

2.8. *Physical measurements*

Elemental analyses (C, H, and N) were performed in a Perkin-Elmer 240 CHNS/O analyzer. Infrared spectra were measured with a Jasco IR report-100 and Shimadzu (IR Prestige-21) FT-IR spectrophotometer using KBr pellets. Far infrared spectra were recorded with a Bruker IFS 66 V spectrometer using polyethylene pellets. Thermal analysis was carried out using Shimadzu DTG-60 TG/DTA apparatus and Shimadzu DSC-60 differential scanning calorimeter. Static susceptibility measurements were made with the help of a Princeton Applied Research Vibrating Sample Magnetometer Model 155. Electronic spectra were recorded with a Jasco V-570 UV/Vis/NIR spectrophotometer using a pair of matched quartz cells of 1 cm path length. Conductivity and pH measurements were done using a Mettler Toledo dual conductivity/pH meter model SevenMulti equipped with Inlab 730 and Inlab 413 electrodes. Electrochemical measurements were done with a PAR Versastat-II electrochemistry system at 298 K under nitrogen. A standard three-electrode cell consisting of a glassy carbon working electrode, a platinum auxiliary electrode and a Ag/AgCl reference electrode was used. TEAP was used as a supporting electrolyte. EPR spectra were recorded using a Varian E-112 X/Q-band spectrometer. Instrumental parameters: modulation frequency = 100 kHz, modulation amplitude = 1 G, microwave power = 20 mW. RT solution EPR spectra were recorded using an aqueous cell. LNT frozen glass EPR spectra were recorded in liquid nitrogen using a quartz dewar. Diphenylpicrylhydrazyl (DPPH) was used as internal field marker.

2.9. *X-ray crystallography for [Cr(NCS)$_2$(salophen)] (2)*

A reddish–brown crystal directly obtained from reaction of **1** with dry KSCN in methanol with approximate size of $0.2 \times 0.15 \times 0.08$ mm^3 was mounted on a Bruker Axs Kappa Apex2 diffractometer equipped with graphite-monochromated [Mo-Kα, $\lambda = 0.71073$ Å] radiation. Unit cell parameters were determined by the method of difference vectors using reflections scanned from three different zones of the

reciprocal lattice. The intensity data were measured using ω and φ scan with frame width of 0.5°. The frames integration and data reduction were performed using Bruker SAINT-Plus (Version 7.06a) software [30]. Multi-scan absorption corrections were applied to the data using SADABS. The crystal is indexed in triclinic system with lattice parameters $a = 8.5820(2)$ Å, $b = 10.6367(3)$ Å, $c = 13.0420(4)$ Å, $\alpha = 81.623(1)°$, $\beta = 87.061(1)°$, $\gamma = 89.073(1)°$. SIR-92 program [31] was used for solving the structure. Structure was refined using SHELXL-97 [32]. The solved structure showed an unknown organic cluster containing sulfur, which was severely disordered. As it was too difficult to segregate the disordered components of the cluster, it was decided to remove its contribution from intensity data using the SQUEEZE program of PLATON [33]. The squeezed data were used for further refinement. The SQUEEZE result showed that the removed cluster contained 81 electrons equivalent of scattering material per unit cell. The unit cell contents and molecular formula reported does not contain contribution from the cluster. The successive difference Fourier map showed the positions of all hydrogen atoms. However, the hydrogen positions were geometrically fixed and refined through a riding model. Full matrix structure refinement was carried out through minimization of the function $\sum(w(F_o^2 - F_c^2))^2$, where $w = [\sigma(F_o^2) + (0.0613P)^2 + 0.7109P]^{-1}$ and $P = (F_o^2 + 2F_c^2)/3$, F_o^2 is the measured intensity (i.e. intensity observed) and F_c^2 is the intensity calculated. The final residual factors were $R = 0.0388$ and $wR = 0.1040$. The largest difference map peak was $0.845\,e\,Å^{-3}$.

3. Results and discussion

3.1. *Thermal analysis and magnetic moments*

Complex **1** decomposes at 350°C, as judged by combined DSC/TGA thermal analysis (Supplementary material), indicating good thermal stability. The RT (at 25°C) magnetic susceptibility measurements show that μ_{eff} values for **1** and **2** are 2.79 and 2.80 BM, respectively, while that for **3** is 3.70 BM. Since the spin–orbit coupling constant value reported for Cr(IV) in the literature [34] is around $160\,cm^{-1}$, we can interpret the RT susceptibility values for **1** and **2** as indicating two unpaired electrons with ^3F ground state for the free ion and hence a $^3T_{1g}(F)$ for these two complexes (in O_h) [35–37]. However, these complexes as indicated by their electronic spectra are expected to be tetragonal with D_{4h} symmetry, and the $^3T_{1g}$ (in O_h) will be split into ^3E_g and $^3A_{2g}$ (in D_{4h}) [36]. Thus, in D_{4h} symmetry, d_{xz}, d_{yz} transform as E_g containing an electron in each orbital. On the other hand, the RT magnetic moment value for **3** indicates the presence of three unpaired electrons for this six-coordinate tetragonal Cr(III) complex with a $^4B_{1g}$ ground state [23, 37, 38] in D_{4h} symmetry (a $^4A_{2g}$ ground term in O_h).

The dark brown to black **1** is readily soluble in CH_3OH, C_2H_5OH, CH_3CN, and DMF, poorly soluble in CH_2Cl_2, and insoluble in water and toluene. Conductivity measurement of **1** in CH_3CN reveals the non-electrolyte nature of the compound. Based on its elemental analysis and conductivity measurement, the compound may be formulated as either [O=Cr(OH$_2$)(salophen)] or its tautomer [Cr(OH)$_2$(salophen)]. The magnetic moment value and EPR results along with the results obtained from the reactions of the compound with different reagents (*vide infra*) strongly suggest the [Cr(OH)$_2$(salophen)] formulation for **1**. It should be pointed out here that though we

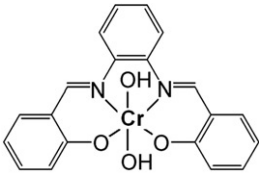

Scheme 1. Structure of **1**.

followed a very similar method of preparation for this compound (reacting ligand with $K_2Cr_2O_7$ in methanol at RT maintaining the stoichiometric ratios), as that was reported for the compound with salen [24], to our surprise the pH of the mother filtrate after completion of the reaction in the case of salophen was found to be ~8, indicating that the protons released by the salophen ligand upon coordination to the metal ion were totally consumed in spite of no external base added, suggesting additional reactions. This could be the key point for the formation of the dihydroxy form of the compound with this salophen ligand, which is found to be very stable under the experimental condition and is isolated as a solid. Thus, based on its elemental analysis, IR spectrum, magnetic moment, and conductivity measurement, and in analogy [3, 13] to $[Cr(OH_2)_2(salophen)]^+$, the proposed structure for **1** is shown in scheme 1. Similar structure has been proposed by Gould [20] for the *trans*-dihydroxyCr(IV) compound $[Cr^{IV}(OH)_2(EHBA)_2]$, where EHBA = 2-ethyl-2-hydroxybutanoate anion. Evidence in support of this *trans*-dihydroxy structure comes from the crystal structure of its *trans*-diisothiocyanato analog $[Cr(NCS)_2(salophen)]$ (**2**) (*vide infra*).

3.2. *Electronic spectra*

The electronic spectra of $[Cr(OH)_2(salophen)]$ (**1**) have been recorded in CH_3CN as well as in DMF and CH_3OH while that for **2** and **3** have been recorded in CH_3OH and CH_3CN solutions. The spectrum of **1** in CH_3CN is shown in figure 1 and the electronic spectral band positions of **1** in CH_3CN and DMF are listed in table 1.

In the electronic spectrum of **1** in CH_3CN the three lowest energy bands at 595, 550, and 480 nm in the visible region are absent in the spectrum of free H_2salophen. The bands at 595 and 550 nm appear almost in the same positions when the spectrum was recorded in DMF, but the band centered at 480 nm ($\varepsilon = 1267$) exhibits a large solvatochromic shift to 464 nm ($\varepsilon = 1874$) in DMF, indicative of charge transfer (CT) character [39]. Similarly the band at 373 nm ($\varepsilon = 3588$) in CH_3CN is shifted to 365 nm ($\varepsilon = 4808$) in DMF, indicating CT character. Weak bands at 595 nm ($\varepsilon = 116$) and 550 nm ($\varepsilon = 212$) may be assigned to $d \rightarrow d$ transitions [23, 37, 38]. The other expected $d \rightarrow d$ transitions [37, 38] are probably masked by the strong CT transitions. When the spectrum is recorded in CH_3OH, two lower energy bands are clearly observed at ~590 nm ($\varepsilon = 127$) and 550 nm ($\varepsilon = 201$), which may be assigned as $d \rightarrow d$ transitions, while the CT band in the visible region is further blue shifted to 456 nm ($\varepsilon = 4247$). Such blue shift in the CT band with increasing solvent polarity was observed in the visible region for [Ni(salen)] and [Ni(salophen)] complexes studied by Di Bella *et al.* [39]. The higher energy bands in the region between 205 and 320 nm observed for **1** are

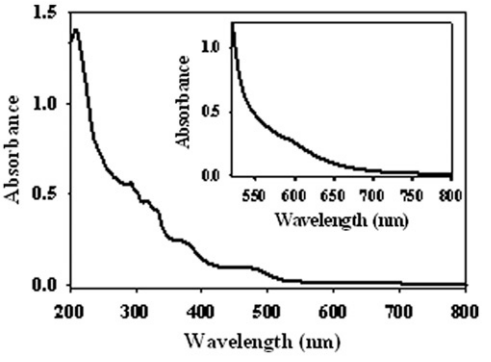

Figure 1. Electronic spectrum of $[Cr(OH)_2(salophen)]$ (**1**) (0.07×10^{-3} mol L^{-1}) in CH_3CN. Inset: concentration 2.25×10^{-3} mol L^{-1}.

Table 1. Electronic spectral band positions in nm (cm^{-1}) of $[Cr(OH)_2(salophen)]$ (**1**) in (a) CH_3CN, (b) DMF.

a				b			
Band positions				Band positions			
nm	(cm^{-1})	ε (mol L^{-1} cm^{-1})	Assignments	nm	(cm^{-1})	ε (mol L^{-1} cm^{-1})	Assignments
595	(16,807)	116	$d \rightarrow d$	595	(16,807)	117	$d \rightarrow d$
550	(18,182)	212	$d \rightarrow d$	548	(18,248	218	$d \rightarrow d$
480	(20,833)	1267	CT	464	(21,552)	1874	CT
373	(26,810)	3588	CT	365	(27,397)	4808	CT
330	(30,303)	6405	$n \rightarrow \pi^*$	332	(30,120)	8153	$n \rightarrow \pi^*$
316	(31,646)	7074	$\pi \rightarrow \pi^*$	318	(31,447)	8868	$\pi \rightarrow \pi^*$
292	(34,247)	8683	$\pi \rightarrow \pi^*$	302	(33,113)	9512	$\pi \rightarrow \pi^*$
207	(47,619)	20,025	$\pi \rightarrow \pi^*$	293	(34,130)	10,482	$\pi \rightarrow \pi^*$

comparable to those in free H_2salophen spectrum and are associated with principally intraligand $\pi \rightarrow \pi^*$ transitions [39].

In the UV-Vis spectrum of the reported chromium(III) complex with the same ligand salophen, $[Cr(OH_2)_2(salophen)]O_3SCF_3$, the two lowest energy bands were observed [3] at 476 nm ($\varepsilon = 6210$) and 342 nm ($\varepsilon = 19{,}400$) while that for $[Cr(OH_2)_2(salophen)]BF_4$ were observed [13] at 469 nm ($\varepsilon = 10{,}400$) and 334 nm ($\varepsilon = 25{,}400$), respectively, clearly indicating the difference in electronic structure of the Cr(III) ion in these two complexes with that of **1** containing a Cr(IV) ion.

To ascertain the structure of **1**, we carried out the following reactions in solutions. When reacted with two fold excess of KSCN or imidazole (imz) in CH_3OH at RT, immediate change in the electronic spectra were observed and the CT band at 456 nm ($\varepsilon = 4247$) in CH_3OH was shifted to 463 and 465 nm in the presence of KSCN and imidazole, respectively. The reaction with KSCN was also followed by pH measurement. The reaction of a 1.25×10^{-3} mol L^{-1} CH_3OH solution of **1** with solid KSCN (1 : 2 ratio) shows an increase in pH resulting in a final pH ~8. This observation strongly suggests the formulation $[Cr(OH)_2(salophen)]$ for **1** based on the following

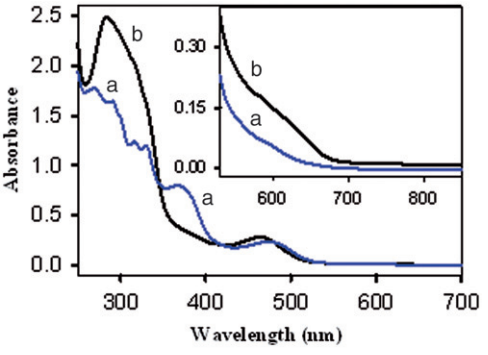

Figure 2. Electronic spectra of $[Cr(NCS)_2(salophen)]$ (**2**) (0.067×10^{-3} mol L^{-1}) (blue curve a) and $K[Cr(NCS)_2(salophen)] \cdot H_2O$ (**3**) (0.115×10^{-3} mol L^{-1}) (black curve b) in CH_3CN. Inset concentration: 0.829×10^{-3} mol L^{-1} for **2**, 1.483×10^{-3} mol L^{-1} for **3**.

reaction with NCS^- that forms *in situ* $[Cr(NCS)_2(salophen)]$ (**2**) and OH^- ions, thus increasing the pH of the solution.

$$\left[Cr(OH)_2(salophen)\right] + 2NCS^- \rightarrow \left[Cr(NCS)_2(salophen)\right] + 2OH^- \qquad (1)$$

This isothiocyanato product $[Cr(NCS)_2(salophen)]$ (**2**) has been synthesized (Section 2) and isolated in solid, purified and its spectra recorded. The appearance of a very strong ν(C=N) band at 2104 cm^{-1} along with a shoulder at 2088 cm^{-1} in its IR spectrum (Supplementary material) strongly suggests the presence of the isothiocyanate ligands [26] and this is confirmed from its X-ray crystal structure (*vide infra*). The ν(C=N) for the reported Cr(III) compound $(Bu_4N)[Cr(NAOP)(NCS)_2]$ ($NAOP^{2-}$ = *N*,*N*′-(1,2-phenylenebis(nitrilomethylidyne))bis(2-naphtholate) were observed at 2061 s and 2089 m cm^{-1}, respectively, while ν(C=N) bands for $(Bu_4N)[Cr(salen)(NCS)_2]$ were observed at 2078 s and 2102 m cm^{-1}, respectively [40]. On the other hand, only one strong ν(C=N) band was observed [40] for $[TTF][Cr(NAOP)(NCS)_2]$ (where TTF = tetrathiafulvalene) at 2071 s cm^{-1} and for $[Cr(salen)(NCS)_2K \cdot H_2O]$ at 2045 cm^{-1} [27]. We have also synthesized the Cr(III) complex $K[Cr(NCS)_2(salophen)] \cdot H_2O$ (**3**) following the reported methods [27–29] and recorded its spectra to get an insight about the difference in its electronic structure with that of **2**. Compound **3** also, like $[Cr(salen)(NCS)_2K \cdot H_2O]$ displays only one strong ν(C=N) band at 2079 cm^{-1} in its IR spectrum. As expected, this band is at much lower frequency than those observed for **2**.

The electronic spectrum of $[Cr(NCS)_2(salophen)]$ (**2**) in CH_3OH (Supplementary material) shows two lower energy d → d transitions at 582 nm ($\varepsilon = 44$) and 545 nm ($\varepsilon = 111$), respectively, while the CT band in the visible region is observed at 463 nm ($\varepsilon = 2793$). This latter band shifted to 473 nm when the spectrum was recorded in CH_3CN. The corresponding Cr(III) compound, $K[Cr(NCS)_2(salophen)] \cdot H_2O$ (**3**), displayed a strong CT band at 464 nm in CH_3CN, and this band was shifted to 459 nm when recorded in methanol. Thus, the difference in the electronic structures of **2** and **3** is clearly reflected from their overall electronic spectra shown in figure 2. Conductance measurements show **2** is a non-electrolyte in CH_3CN while the Cr(III) complex, $K[Cr(NCS)_2(salophen)] \cdot H_2O$ (**3**), is a 1 : 1 electrolyte ($\Lambda = 120$ Ohm^{-1} cm^2 mol^{-1}) in the

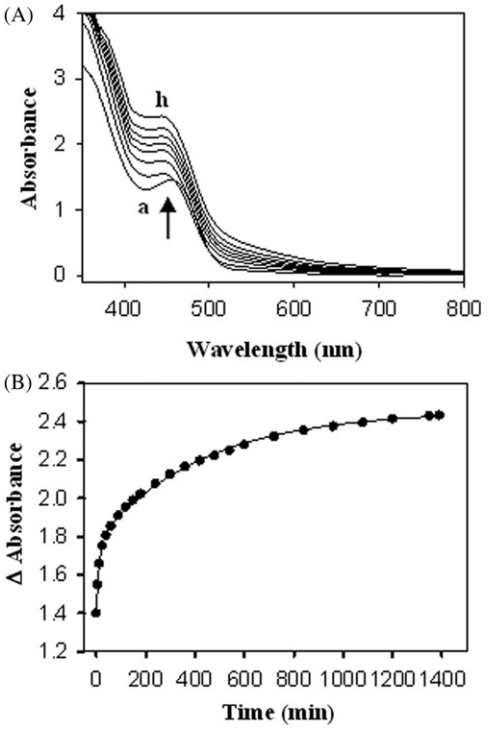

Figure 3. (A) Electronic spectral change for the reaction of $[Cr(OH)_2(salophen)]$ (**1**) (0.34×10^{-3} mol L^{-1}) in CH_3OH with two fold excess of solid $Mn(OAc)_2$ at RT. (a) in the absence of Mn^{2+}, (h) near completion of the reaction with Mn^{2+}. (B) Plot of absorbance change at 443 nm with time (dark circles) along with its two exponential fit (solid line) using the equation $\Delta A_t = c + a_1(1 - e^{-k_1 t}) + a_2(1 - e^{-k_2 t})$.

same solvent [41]. Formation of **2** from reaction of **1** with KSCN in methanol at RT strongly indicates *trans*-dihydroxy structure of **1**, and not the $[O{=}Cr(OH_2)(salophen)]$, because it is highly unlikely that the strongly bonded *oxo* group is simply replaced by NCS^- at RT. **1** did not react with PPh_3, even at warmed condition, and no formation of $O{=}PPh_3$ was detected. This strongly suggests that this compound does not contain a Cr=O group. Both **1** and **2** are stable in solution and no uncatalyzed disproportionation is observed in solution in contrast to other reported Cr(IV) species that spontaneously undergo uncatalyzed disproportionation [20a, c]. However, both these compounds undergo Mn^{2+} catalyzed disproportionation as described below.

We have carried out reaction of **1** and its isothiocyanato and imidazole analogs in CH_3OH at RT with Mn^{2+} ion which is known as a Cr(IV)-specific reductant [20, 42, 43]. It was found that **1** (and also the other two analogs) readily reacts with $Mn(OAc)_2$ as evident from the electronic spectral change with time shown in figure 3. Addition of NaOAc instead of $Mn(OAc)_2$ to CH_3OH solution of **1** causes only slight shift in the band positions, e.g., from 456 to 453 nm, similar to those observed in the cases of addition of imidazole and NCS^- discussed earlier, but there is no further spectral change with time. This clearly suggests that the spectral change shown in figure 3 originates from reaction of Mn^{2+} with **1**. The absence of an isosbestic point in figure 3

Table 2. Kinetic parameters for the reaction of **1**, **2**, and **4** with Mn(II) in CH_3OH at RT.

	Complex **1**	Complex **2**	Complex **4**[a]
Constant c	1.4067	1.4661	1.0641
a_1	0.3705	0.2715	0.3121
k_1 (min^{-1})	0.0782	0.1154	0.0791
a_2	0.6757	0.4393	0.7203
k_2 (min^{-1})	0.0023	0.0029	0.0023
a_1/a_2	0.5483	0.6180	0.43329
k_1/k_2	34.0	39.79	34.39

Data for the plot of absorbance change at λ_{max} with time were fitted using the equation $\Delta A_t = c + a_1(1 - e^{-k_1 t}) + a_2(1 - e^{-k_2 t})$. For **1**, $\lambda_{max} = 443$ nm; for **2**, $\lambda_{max} = 450$ nm, and for **4**, $\lambda_{max} = 455$ nm.
[a]This was generated *in situ* from reaction of **1** with imidazole (1 : 2) in CH_3OH at RT.

suggests the presence of more than two species in appreciable amounts in solution. The CT band at 456 nm of **1** in CH_3OH (figure 3, curve a) shifts to 443 nm with increased absorbance on reaction with Mn^{2+} (figure 3, curve h). Similarly, the CT band for $[Cr(NCS)_2(salophen)]$ (**2**) shifts from 463 to 450 nm and that for $[Cr(imz)_2(salophen)]^{2+}$ (**4**), which was generated *in situ*, shifts from 465 to 455 nm with increased absorbance on reaction with Mn^{2+} (figures not shown). However, the reaction of **1** or its isothiocyanato or imidazole derivative with Mn^{2+} is very slow and in each case takes more than 24 h to complete the reaction at RT in CH_3OH.

Data for the plot of absorbance changes at λ_{max} with time were fitted using the two exponential model

$$\Delta A_t = c + a_1(1 - e^{-k_1 t}) + a_2(1 - e^{-k_2 t}) \quad (2)$$

in each case and the parameters are presented in table 2. The k_1 is higher in the isothiocyanate complex **2** compared to the other two cases which have nearly the same k_1 values. However, in all the three cases, a very slow component is observed with very similar rate constant (k_2). This two-step kinetic profile may be explained based on the mechanism of Mn^{2+} catalyzed disproportionation of *trans*-dihydroxy Cr^{IV} compound $[Cr^{IV}(OH)_2(EHBA)_2]$ in aqueous medium proposed by Gould and his coworkers [20a, 43] who suggested that the principal route utilizes the activated complex Cr^{IV}–OH–Mn^{II} as shown below.

$$Cr^{IV}(OH) + Mn^{II} \rightleftharpoons Cr^{IV}{-}OH{-}Mn^{II} \rightarrow Cr^{III}{-}OH + Mn^{III} \quad (3)$$

$$Cr^{IV}(OH) + Mn^{III} \rightleftharpoons Cr^{IV}{-}OH{-}Mn^{III} \rightarrow Cr^{V}{-}OH + Mn^{II} \quad (4)$$

A similar mechanism may be invoked in the present cases in CH_3OH also and it is likely that the rate of the secondary route involving the Mn(III) species is much different from that of the principal route [20c] and these should account for the two kinetic components observed in all these cases.

Many chromium compounds are responsible for chromium-induced carcinogenicity [20b]. It is also reported that hexavalent chromium itself does not react readily with the isolated DNA, but the reduction of hexavalent chromium to its lower oxidation states Cr(V) and/or Cr(IV) by cellular reductants has been considered an important step

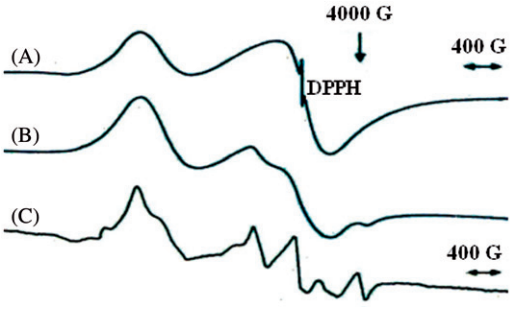

Figure 4. EPR spectra of $[Cr(OH)_2(salophen)]$ (**1**) recorded at X-band frequency (A) powder at RT with DPPH, (B) powder at LNT without DPPH, and (C) frozen glass in DMF at LNT without DPPH.

toward chromium induced carcinogenicity [20b, c]. Thus, it will be important to study the interaction of any chromium compound in its oxidation state of Cr(V) or Cr(IV) with DNA. We have not studied the interaction of our compounds with DNA yet, and we plan to perform these studies in the future, because it is believed that chromium(IV) interaction with DNA is responsible for carcinogenesis [20b, c].

3.3. *EPR results*

The powder EPR spectra for **1** were recorded at X-band frequency both at RT and LNT (figure 4A, B) and also at Q-band frequency at RT (figure 5). When this compound is dissolved in DMF, the solution does not exhibit any EPR signal at RT. However, when this DMF solution is frozen as a glass at LNT, strong EPR signal is observed (figure 4C). Powder EPR spectra for **2** were recorded at X-band frequency, both at RT and LNT. This compound displayed a broad signal at LNT. The frozen glass LNT spectrum of **2** in methanol was also very broad and similar to that observed for its powder LNT spectrum (figures not shown). This indicates that it is a paramagnet with fast relaxation.

The powder spectra displayed by **1** at X-band, both at RT and LNT, are very broad, the latter, however, getting resolved for dipolar splitting at LNT. The g values calculated from the RT powder spectrum are 2.0038 and 4.2080 for **1**. The EPR of the chromium(IV) complexes can be interpreted [24] by the simple Spin Hamiltonian,

$$\mathrm{H} = \beta \mathbf{B} \cdot \mathbf{g} \cdot \mathbf{S} + \mathbf{S} \cdot \mathbf{D} \cdot \mathbf{S} \tag{5}$$

with $\mathbf{S} = \mathbf{1}$, $\mathbf{g}$ and $\mathbf{D}$ being tensors and the contributions from hyperfine interaction being neglected. Compound **1** has been studied using powder both at RT and LNT (figure 4A and B) and frozen DMF solution (figure 4C) at LNT in X-band, and powder at RT in Q-band (figure 5). Measurement at two different frequencies gives understanding of the origin of these unusually broad lines. The RT and LNT powder spectra in X-band clearly exhibit two lines, one at $g = 2.0038$ and the other at $g = 4.2080$ that could be termed as a half-field line. The first line at $g = 2.0038$ corresponds to the $|0> \leftrightarrow |\pm 1>$ transition from the Kramers doublet $|\pm 1>$. However, the broad and intense line at low field, i.e. with the g-value of 4.2080 is due to the forbidden transition $|-1> \leftrightarrow |+1>$. While the large intensity is caused by fairly large D value, substantial

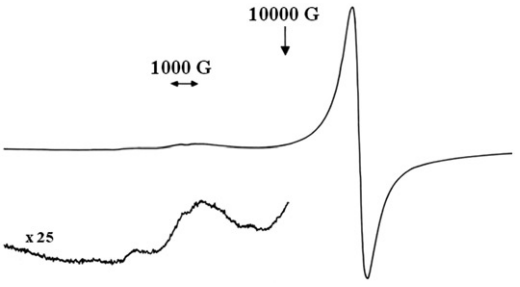

Figure 5. Powder EPR spectrum of $[Cr(OH)_2(salophen)]$ (**1**) recorded at Q-band frequency at RT without DPPH.

broadening could be caused by dipolar interaction between nearby paramagnetic species, noting that the powder is a condensed paramagnetic lattice. It is to be noted, however, that the allowed line partially resolves to reveal the $2D$ separation at LNT (figure 4B).

The dipolar splitting observed in the LNT spectrum of the powder was further confirmed by the even better resolved LNT spectrum of the DMF solution. This X-band LNT frozen glass spectrum which corresponds to a six-line polycrystalline spectrum (figure 4C) is very similar to the X-band LNT frozen glass spectrum of the reported [23] Cr(IV) compound $[Cr(abtsal)_2]$ in DMF and shows the presence of zero-field split rhombic symmetry, indicating a $2D$ separation of 1440 G, $D+E$ of 970 G, and $D-E$ of 470 G. The resulting parameters are $g \cong 2.0$, $D = 720$ G, $E = 250$ G in the present case. These large D and E values should be due to large deviations from the octahedral geometry of this molecule having been subjected to Jahn–Teller distortions. So, it is not surprising that the intensity of $\Delta M_s = \pm 2$ forbidden transition is large due to the large D value. Another possibility of assigning the two lines corresponding to "$\Delta M_s = \pm 1$" and "$\Delta M_s = \pm 2$", as described above, can be interpreted as $g_\perp$ and $g_{||}$, respectively. The latter interpretation cannot be true since the Q-band EPR spectrum (figure 5) at RT does not show spectral characteristic of a polycrystalline axially symmetric system. The observed Q-band EPR shows similar broadening characteristic for the $g \cong 2.0$ line ($\Delta M_s = \pm 1$) with more broadening at the wings with $\Delta B_{pp} \cong 500$ G. However, the $\Delta M_s = \pm 2$ transition gets considerably reduced in intensity, as this behavior is expected in a higher frequency EPR measurement of an $S = 1$ system.

3.4. *Electrochemical results*

The redox behavior of **1** has been studied in CH_3CN containing 0.1 mol L^{-1} TEAP at a glassy carbon working electrode, platinum auxiliary electrode, and a Ag/AgCl reference electrode using cyclic voltammetry. The cyclic voltammogram shows cathodic waves at -0.84 and -1.63 V, respectively (figure 6). The shapes and positions of these waves are not affected by variable scan rates (figure not shown), indicating high reproducibility of the electrode reaction. The reductive response at -1.63 V is coupled to an anodic peak at -1.54 V ($\Delta E_P = 90$ mV) suggesting a quasi reversible electron transfer process for this step.

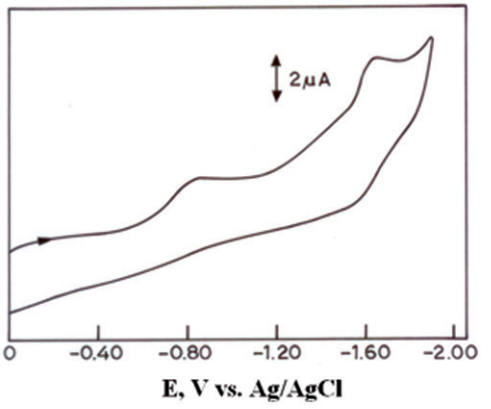

Figure 6. Cyclic voltammogram of $[Cr(OH)_2(salophen)]$ (**1**) (1.0×10^{-3} mol L^{-1}) in CH_3CN containing 0.1 mol L^{-1} TEAP at a scan rate of 100 mV s^{-1}.

For an initial positive scan, on the other hand, two anodic waves were observed at +1.03 and +1.47 V, respectively. No corresponding cathodic peaks were observed on scan reversal (figure not shown). Moreover, these two anodic waves were not observed in the second cycle and a second cycle yields only a very broad oxidation wave around +1.50 V with large anodic current indicating oxidative degradation of the compound followed by electrode pollution. This is not surprising because the transient oxochromium(V)salophen compound generated in CH_3CN from the chemical oxidation of the $[Cr^{III}(OH_2)_2(salophen)]^+$ complex was also found to be unstable in solution and readily precipitated as a sparingly soluble solid [3].

Ortiz and Park [44] have studied the redox behavior of $[Co^{II}(salophen)]$ in DMSO using cyclic voltammetry and coulometry and reported two nearly reversible redox couples at 0.051 and −1.03 V (*vs.* Ag/AgCl) corresponding to Co(III)/Co(II) and Co(II)/Co(I), respectively. Thus, the first reduction observed at −0.84 V (*vs.* Ag/AgCl) for **1** in the present case is associated with metal-centered reduction. The free ligand is not reduced at this potential. Isse *et al.* [45] have shown from their electrochemical studies for the reduction of H_2salophen (H_2L) in DMF using cyclic voltammetry, coulometry, and controlled potential electrolysis that H_2L undergoes two-electron reduction at a potential −1.53 V (*vs.* SCE) while the monoanion (HL^-) is reduced at *ca*, −1.65 V and the dianion (L^{2-}) is reduced at *ca*, −2.47 V, respectively. The reduction of H_2salophen in DMF involved a self-protonation mechanism, whereby the conjugate bases HL^- and L^{2-} were produced as a consequence of the proton transfer from the substrate to the basic reduction intermediates. The same researchers also studied [46, 47] the electrochemical reductions of $[Ni^{II}(salophen)]$ and $[Co^{II}(salophen)]$ in DMF. In the case of [Ni(salophen)], the first step was [46] a ligand-based one-electron reduction at −1.39 V (*vs.* SCE) forming a radical anion of the complex, which rapidly led to formation of a C–C bond between two complex radical anions resulting in a new dimeric compound. This dimer underwent a metal-centered reversible reduction at −2.25 V. [Co(salophen)] showed [47] three successive reductions, each involving a one-electron process. The first step was a metal-centered reduction whereas the last two steps were ligand-based reductions which led to the formation of a new cobalt complex that had a Co(II)/Co(I) redox couple located at a potential 600 mV negative to that of

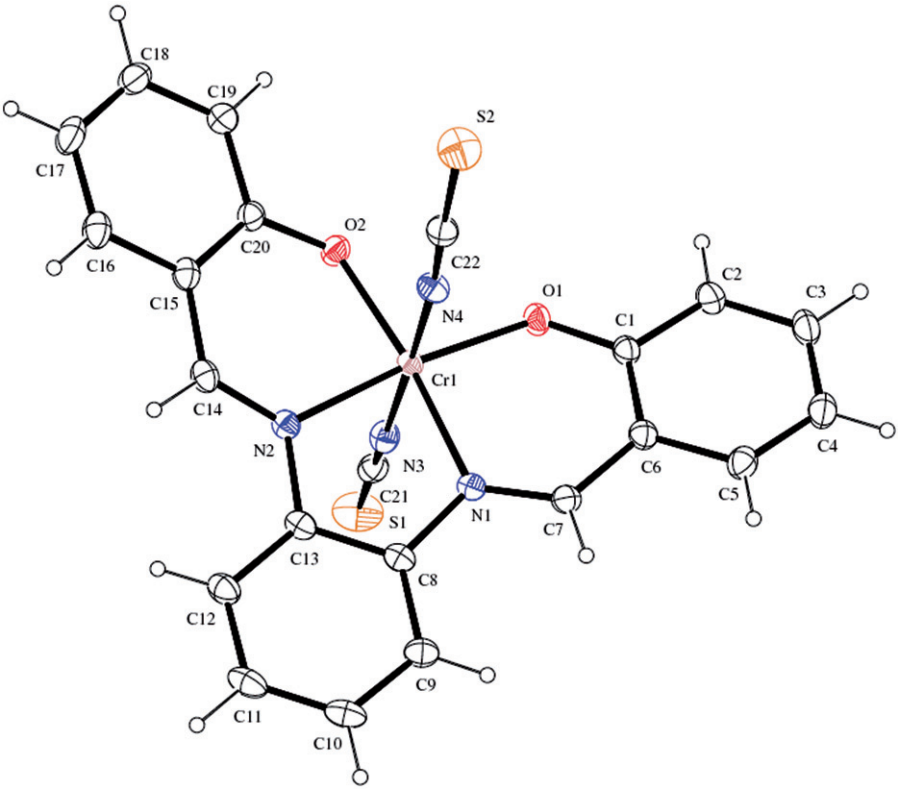

Figure 7. ORTEP diagram of $[Cr(NCS)_2(salophen)]$ (**2**). Selected bond lengths (Å) and angles (°): N(1)–Cr(1), 2.011(2); N(2)–Cr(1), 2.0139(19); N(3)–Cr(1), 2.032(2); N(4)–Cr(1), 2.015(2); O(1)–Cr(1), 1.9290(16); O(2)–Cr(1), 1.9318(17); O(1)–Cr(1)–O(2), 95.11(7); O(1)–Cr(1)–N(1), 92.14(8); O(2)–Cr(1)–N(2), 91.75(8); N(1)–Cr(1)–N(2), 81.01(8); O(2)–Cr(1)–N(1), 172.73(7); O(1)–Cr(1)–N(2), 173.13(8); N(4)–Cr(1)–N(3), 178.45(9).

the original complex. Thus, in $[Ni^{II}(salophen)]$ and $[Co^{II}(salophen)]$, the ligand-centered reduction resulted in new species, which underwent further reduction at a different potential than the initial species. Formation of no such new species is observed in the electrochemical reduction of **1** under the present experimental conditions, suggesting that the cathodic wave at −1.63 V (*vs.* Ag/AgCl) for **1** is possibly associated with metal-centered reduction, though the possibility of ligand-centered reduction is not completely ruled out at this potential. Thus, the quasi-reversible step in the present case at $E_{1/2}(red) = -1.585$ V is most likely due to a Cr(III)/Cr(II) couple. Similar quasi-reversible Cr(III)/Cr(II) couples are reported for a number of $[Cr(OH_2)_2(salen)]^+$ complexes in DMSO where the observed half-wave potentials were −1.31 to −1.41 V (*vs.* SCE) [48, 49].

3.5. *Crystal structure of [Cr(NCS)$_2$(salophen)] (2)*

The structure of **2** has been determined by X-ray crystallography. Figure 7 shows the ORTEP representation of the molecule with 40% probability ellipsoids [50].

The geometry around Cr(IV) is distorted octahedral. The two Cr–N bond lengths in the equatorial plane are very close (N(1)–Cr(1), 2.011(2); N(2)–Cr(1), 2.0139(19)) while the two axial Cr–N bond lengths are slightly different (N(3)–Cr(1), 2.032(2); N(4)–Cr(1), 2.015(2)) from each other. The two Cr–O bond lengths are almost equal (O(1)–Cr(1), 1.9290(16); O(2)–Cr(1), 1.9318(17)) and considerably shorter than any of the four Cr–N bond lengths. Apparently, the ligand is puckered (Supplementary material) in **2** as evidenced from the dihedral angles between phenylene planes (I) C1,C2,C3,C4,C5,C6; (II) C8,C9,C10,C11,C12,C13; (III) C15,C16,C17,C18,C19,C20. The respective dihedral angles between mean planes are 16.27(6) (I and II), 32.60(8) (I and III), 22.67(10) (II and III) degrees, respectively. The bond angles O(2)–Cr(1)–N(1) = 172.73(7) and O(1)–Cr(1)–N(2) = 173.13(8) indicate that O–Cr–N bonds are nonlinear; on the other hand N(4)–Cr(1)–N(3) bond angle is 178.45(9). The Cr–N bond distances for *trans*-NCS in **2** are remarkably similar to those (2.030(3) and 2.018(3) Å) reported for [TTF][Cr(NAOP)$(NCS)_2$], where TTF = tetrathiafulvalene [40]. In this reported compound, the Cr is six-coordinate with tetradentate $NAOP^{2-}$ in the equatorial plane and two NCS^- in axial positions coordinated *via* N; the Cr–N and Cr–O ($NAOP^{2-}$) distances were in agreement with those observed in other [27] Cr(III) Schiff-base complexes but the axial Cr–N bonds are slightly longer than those observed for [Cr(salen)$(NCS)_2 K \cdot H_2O$] though both contain Cr(III). It appears that the nature and structure of the Schiff-base ligand have some influence on the axial Cr–N bond distances in these reported compounds. Thus, it is a coincidence that the axial Cr–N bond distances in the present case are similar to those in [TTF][Cr(NAOP)$(NCS)_2$], though the metal ion oxidation states are different in the two cases. The ν(C=N) band at 2071s cm^{-1} for this reported complex [40] is at lower frequency than that observed for **2** as expected for the difference in their metal ion oxidation states.

4. Conclusions

It has been possible to stabilize and isolate a paramagnetic *trans*-dihydroxy Cr(IV) complex [Cr$(OH)_2$(salophen)] (**1**) in the solid state with H_2salophen having π-delocalization. The compound is stable in solid as well as in solution in the presence of air. The compound exhibits powder EPR spectra at RT and at LNT, as well as in frozen glass at LNT. Several attempts to prepare single crystals for this Cr(IV) compound were unsuccessful, so X-ray structural determination was not possible and all the studies were confined to powders and solutions. However, it has been possible to get single crystals for the corresponding *trans*-diisothiocyanato complex, [Cr$(NCS)_2$(salophen)] (**2**), and its crystal structure has been determined by X-ray crystallography and found to contain two N-bonded axial thiocyanate ligands. Thus, indirect evidence regarding the *trans*-dihydroxy structure of **1** comes from the crystal structure of its *trans*-diisothiocyanato analog. On the other hand, the formulation of Cr(IV) oxidation state is supported not only by its magnetic moment and EPR results, but also from its reaction in solution with Mn^{2+} ion, a Cr(IV)-specific reductant, and finally from the crystal structure of **2**.

Supplementary material

Figure S1: TGA-DSC diagram for **1**, figure S2: IR spectrum of **2**, figure S3: electronic spectrum of **2**, figure S4: showing the puckering of the ligand in **2**, figure S5: showing the packing of the molecules of **2** in the unit cell. Crystallographic data for the structural analysis for **2** have been deposited with the Cambridge Crystallographic Data Center, CCDC number 835516. These data can be obtained free of charge *via* http://www.ccdc.cam.ac.uk/conts/retrieving.html, or from the Cambridge Crystallographic Data Centre, 12 Union Road, Cambridge CB2 1EZ, UK; Fax: (+44) 1223-336-033; or E-mail: deposit@ccdc.cam.ac.uk.

Acknowledgments

A.P.K. and M.K. thank Prof. Sakti Prasad Ghosh, Department of Inorganic Chemistry, Indian Association for the Cultivation of Science, Kolkata, for help with the elemental analysis and magnetic moment measurements. M.K. thanks Prof. Shyamal Kumar Chattopadhyay of the Department of Chemistry, Bengal Engineering and Science University, Shibpur, Howrah, for providing electrochemical facilities. We thank the SAIF, IIT-Madras for providing XRD, EPR, and far-infrared facilities. A.P.K. thanks Mr Bhanudas Naik, Department of Chemistry, BITS, Pilani – K.K. Birla Goa Campus for help with the thermal analysis and Prof. B.R. Srinivasan, Department of Chemistry, Goa University for help with the IR facility. P.T.M. thanks the DST, Govt. of India for Ramanna Fellowship (SR/S1/RFIC-02/2006) and also the INSA for its Senior Scientistship.

References

[1] W. Adam, F.G. Gelalcha, C.R. Saha-Moeller, V.R. Stegmann. *J. Org. Chem.*, **65**, 1915 (2000).
[2] E.G. Samsel, K. Srinivasan, J.K. Kochi. *J. Am. Chem. Soc.*, **107**, 7606 (1985).
[3] K. Srinivasan, J.K. Kochi. *Inorg. Chem.*, **24**, 4671 (1985).
[4] C. Bousquet, D. Gilheany. *Tetrahedron Lett.*, **36**, 7739 (1995).
[5] C.T. Dalton, K.M. Ryan, V.M. Wall, C. Bousquet, D.G. Gilheany. *Topics Catal.*, **5**, 75 (1998).
[6] H. Imanishi, T. Katsuki. *Tetrahedron Lett.*, **38**, 251 (1997).
[7] J.F. Larrow, S.E. Schauss, E.N. Jacobsen. *J. Am. Chem. Soc.*, **118**, 7420 (1996).
[8] B.D. Brandes, E.N. Jacobsen. *Synlett*, 1013 (2001).
[9] M. Bandini, P.G. Gozzi, P. Melchiorre, A. Umani-Ronchi. *Angew. Chem. Int. Ed.*, **38**, 3357 (1999).
[10] M. Bandini, P.G. Gozzi, A. Umani-Ronchi. *Angew. Chem. Int. Ed.*, **39**, 2327 (2000).
[11] M. Bandini, P.G. Gozzi, A. Umani-Ronchi. *Tetrahedron*, **57**, 835 (2001).
[12] M. Zintl, F. Molnar, T. Urban, V. Bernhart, P. Preishuber-Pflugl, B. Rieger. *Angew. Chem. Int. Ed.*, **47**, 3458 (2008).
[13] M. Ohashi, T. Koshiyama, T. Ueno, M. Yanase, H. Fujii, Y. Watanabe. *Angew. Chem. Int. Ed.*, **42**, 1005 (2003).
[14] C.M. Thomas, T.R. Ward. *Chem. Soc. Rev.*, **34**, 337 (2005).
[15] T. Ueno, T. Koshiyama, M. Ohashi, K. Kondo, M. Kono, A. Suzuki, T. Yamane, Y. Watanabe. *J. Am. Chem. Soc.*, **127**, 6556 (2005).
[16] W. Adam, S. Hajra, M. Herderich, C.R. Saha-Mo1ller. *Org. Lett.*, **2**, 2773 (2000).
[17] N.S. Venkataramanan, S. Premsingh, S. Rajagopal, K. Pitchumani. *J. Org. Chem.*, **68**, 7460 (2003).
[18] R. Sevvel, S. Rajagopal, C. Srinivasan, N.I. Alhaji, A. Chellamani. *J. Org. Chem.*, **65**, 3334 (2000).
[19] F.A. Cotton, G. Wilkinson, C.A. Murillo, M. Bochmann. *Advanced Inorganic Chemistry*, 6th Edn, Wiley, New York (1999).

[20] (a) E.S. Gould. *Coord. Chem. Rev.*, **135/136**, 651 (1994) and references therein; (b) R. Saha, R. Nandi, B. Saha. *J. Coord. Chem.*, **64**, 1782 (2011) and references therein; (c) M.K. Koley, S.C. Sivasubramanian, S. Biswas, P.T. Manoharan, A.P. Koley. *J. Coord. Chem.*, **65**, 3329 (2012).
[21] J.R. Budge, B.M.K. Gatehouse, M.C. Nesbit, B.O. West. *J. Chem. Soc., Chem. Commun.*, 370 (1981).
[22] J.T. Groves, W.J. Kruper Jr., R.C. Haushalter, W.M. Butler. *Inorg. Chem.*, **21**, 1363 (1982).
[23] M.K. Koley, S.C. Sivasubramanian, B. Varghese, P.T. Manoharan, A.P. Koley. *Inorg. Chim. Acta*, **361**, 1485 (2008) and references therein.
[24] M.K. Koley, P.T. Manoharan, A.P. Koley. *Inorg. Chim. Acta*, **363**, 3798 (2010).
[25] D.T. Sawyer, J.L. Roberts. *Experimental Electrochemistry for Chemists*, Wiley, New York (1974).
[26] K. Nakamoto, *Infrared and Raman Spectra of Inorganic and Coordination Compounds, Part B, Applications in Coordination, Organometallic, and Bioinorganic Chemistry*, 5th Edn, Wiley, New York (1997).
[27] H. Li, Z.J. Zhong, X.-Z. You, W. Chen. *Polyhedron*, **16**, 1119 (1997).
[28] S. Yamada, K. Iwasaki. *Inorg. Chim. Acta*, **5**, 3 (1971).
[29] F. Lloret, M. Julve, M. Mollar, I. Castro, J. Latorre, J. Faus. *J. Chem. Soc., Dalton Trans.*, 729 (1989).
[30] Bruker-Nonius. *APEX-II and SAINT-Plus (Version 7.06a)*, Bruker AXS Inc., Madison, Wisconsin, USA (2004).
[31] A. Altormare, G. Gascarano, C. Giacovazzo, A. Guagliardi. *J. Appl. Cryst.*, **26**, 343 (1993).
[32] G.M. Sheldrick. *SHELXL-97*, University of Göttingen, Germany (1997).
[33] A.L. Spek. *J. Appl. Cryst.*, **36**, 7 (2003).
[34] A. Abragam, B. Bleany. *Electron Paramagnetic Resonance of Transition Ions*, Clarendon Press, Oxford (1970).
[35] F.E. Mabbs, D. Collison. *Electron Paramagnetic Resonance of Transition Metal Compounds*, Vol. 485, Elsevier, Amsterdam (1992).
[36] A.B.P. Lever, E.I. Solomon. In *Inorganic Electronic Structure and Spectroscopy, Vol. I: Methodology*, E.I. Solomon, A.B.P. Lever (Eds), pp. 35–50, Wiley-Interscience, New Jersey (1999).
[37] A.B.P. Lever. *Inorganic Electronic Spectroscopy*, 2nd Edn, Elsevier, New York (1984).
[38] J.E. Huheey, E.A. Keiter, R.L. Keiter. *Inorganic Chemistry: Principles of Structure and Reactivity*, 4th Edn, pp. 438–439, 448–449, Pearson Education, New Delhi, India (2003).
[39] S. Di Bella, I. Fragala, I. Ledoux, M.A. Diaz-Garcia, T.J. Marks. *J. Am. Chem. Soc.*, **119**, 9550 (1997).
[40] S. Wang, P. Day, J.D. Wallis, P.N. Horton, M.B. Hursthouse. *Polyhedron*, **25**, 2583 (2006).
[41] W.J. Geary. *Coord. Chem. Rev.*, **7**, 81 (1971).
[42] K.D. Sugden, K.E. Wetterhahn. *J. Am. Chem. Soc.*, **118**, 10811 (1996).
[43] M.C. Ghosh, E. Gelerinter, E.S. Gould. *Inorg. Chem.*, **31**, 702 (1992).
[44] B. Ortiz, S.-M. Park. *Bull. Korean Chem. Soc.*, **21**, 405 (2000).
[45] A. Ahmed Isse, A. Gennaro, E. Vianello. *Electrochim. Acta*, **42**, 2065 (1997).
[46] A. Ahmed Isse, A. Gennaro, E. Vianello. *Electrochim. Acta*, **37**, 113 (1992).
[47] A. Ahmed Isse, A. Gennaro, E. Vianello. *J. Chem. Soc., Dalton Trans.*, 2091 (1993).
[48] M. Kanthimathi, B. Unni Nair, T. Ramasami, J. Jeyakanthan, D. Velmurugan. *Trans. Met. Chem.*, **25**, 145 (2000).
[49] M. Kanthimathi, B. Unni Nair, T. Ramasami, T. Shibahara, T. Tada. *Proc. Indian Acad. Sci. (Chem. Sci.)*, **109**, 235 (1997).
[50] L.J. Frrugia. *J. Appl. Cryst.*, **30**, 565 (1997).